JOC The Journal of Organic Chemistry

Article

Phenothiazine Decorated Carbazoles: Effect of Substitution Pattern on the Optical and Electroluminescent Characteristics

Rajendra Kumar Konidena, K. R. Justin Thomas, Sudhir Kumar, Ya-Chi Wang, Chieh-Ju Li, and Jwo-Huei Jou

J. Org. Chem., **Just Accepted Manuscript** • Publication Date (Web): 07 May 2015

Phenothiazine Decorated Carbazoles: Effect of Substitution Pattern on the Optical and Electroluminescent Characteristics

Rajendra Kumar Konidena,[a] K. R. Justin Thomas,[a] Sudhir Kumar,[b] Ya-Chi Wang,[b] Chieh-Ju Li[b] and Jwo-Huei Jou[b]*

[a] Organic Materials Laboratory, Department of Chemistry, Indian Institute of Technology Roorkee, Roorkee – 247 667, India

[b] Department of Material Science and Engineering, National Tsing Hua University, Hsinchu 30013, Taiwan

krjt8fcy@iitr.ac.in

Abstract. A series of thienylphenothiazine decorated carbazoles were synthesized and characterized by optical, electrochemical, thermal and theoretical investigations. Absorption spectra of the compounds are influenced by the substitution pattern and chromophore number density. Compounds containing 2,7-substitution exhibited red-shifted absorption while the chromophore loading on the other positions led to the increment in molar extinction coefficients owing to the increase in the chromophore density. Multiple substitutions resulted in twisting of chromophores and affected the conjugative delocalization of the π-electrons which produced shorter wavelength absorption for the 2,3,6,7-tetrasubstituted derivative. Interestingly, the compounds exhibited excited state solvatochromism attributable to the structural reorganization induced electronic perturbations. The solvatochromic data is supportive of a general

solvent effect which is further confirmed by Lippert-Mataga correlation. End-capping with butterfly shaped phenothiazine restrained the formation of molecular aggregates in the solid state. All the compounds displayed exceptional thermal stability attributable to the rigid carbazole building block. Solution processed OLED fabricated using the new materials as emitting dopants in 4,4'-bis(9*H*-carbazol-9-yl)biphenyl host exhibited bluish green electroluminescence.

Keywords: carbazole, phenothiazine, absorption, emission, solvatochromism, density functional theory, organic light emitting diodes.

Graphical Abstract

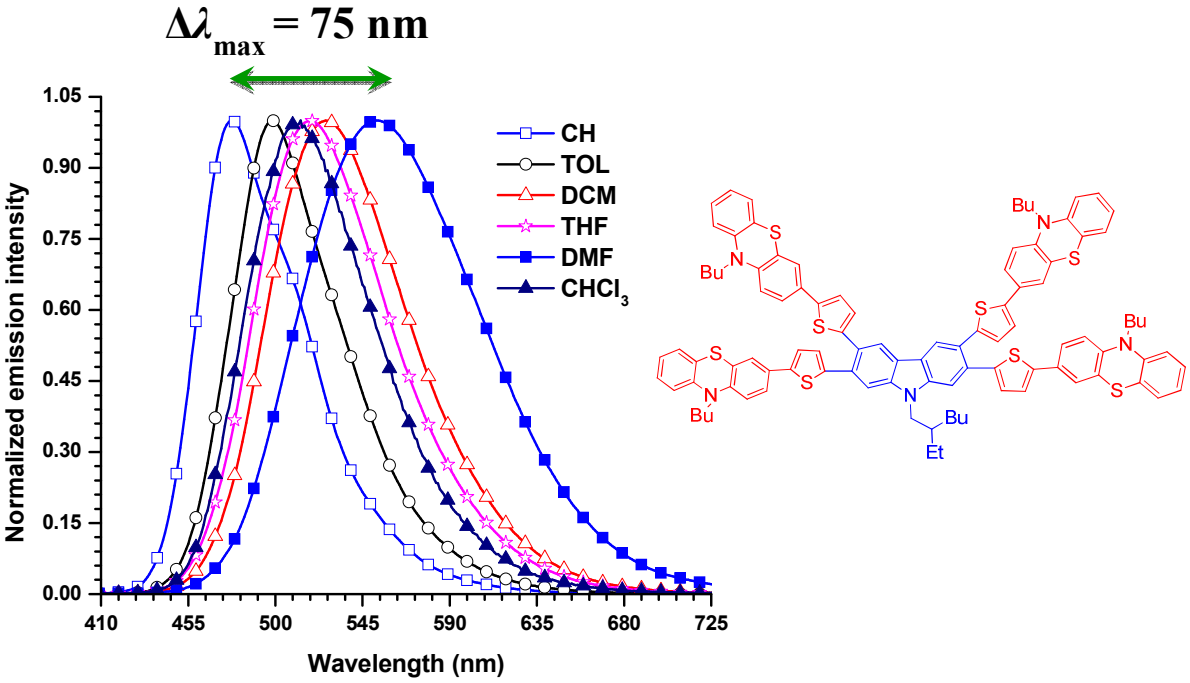

INTRODUCTION

The development of π-conjugated organic materials had drawn immense attention from the scientific community owing to their unique optical and electronic properties. During the past two decades functional materials suitable for application in organic light-emitting diodes (OLEDs) based on small molecules,[1,2] dendrimers[3] and polymers[4] have been actively investigated. Among them, small molecules are attractive due to their well-defined molecular structure, precise control on functional properties of the materials, ability to deliver unachievable purity by polymers, and capability to be processed in solution and vacuum deposition methods.[2] Current focus on OLED research is mainly on device optimization methods, development of pure color emitters (red, green and blue) suitable for solution processable devices, thermal stability, and triplet harvesting strategies such as thermally assisted delayed fluorescence.[5,6] Thus, the development of π-conjugated small molecules and establishment of their structure-property relationships are desirable.[7,8] In this regard, the choice of building blocks should be examined carefully, because they tend to dominate the functional properties of the materials.[8,9] And, also the topological arrangements of the functional units around the central building block influence greatly on physicochemical, thermal and carrier transport properties.[6,9-13] Nevertheless, the systematic studies on the π-conjugated oligomers and their linking topology effects on materials properties deserve more attention. Recently, it has been found that construction of molecular materials with multifunctional building blocks are considered as promising strategy to improve the performance characteristics of light-emitting devices.[14]

In this work, we have chosen to develop materials integrating carbazole and phenothiazine. Among the heterocyclic compounds, 9*H*-carbazole is one of the prototypical molecule and is adopted as a promising building block for many of functional organic materials owing to their rigid molecular structure, availability, amorphous nature, excellent

hole transporting ability, wide scope for functionality and high thermal and photochemical stabilities.[15] Apart from these interesting features, its high triplet energy (2.9 eV) makes it a suitable host for phosphorescent OLEDs (PhOLEDs).[16,17] To date, carbazole and its derivatives are successfully applied in organic light emitting diodes (OLEDs),[9-13,16,17] organic thin film transistors (OFETs),[18] photovoltaic cells,[19,20] photorefractive materials[21] and as receptors in fluorescent sensors.[22] Structurally phenothiazine can be considered as sulfur inserted carbazole.[23] Its unique butterfly configuration and high electron rich character are beneficial for its potential function in optoelectronic applications.[24-28] Recently, Jiang and co-workers reported a potential host material for PhOLEDs by connecting phenothiazine and carbazole by C-N linkage.[25] As a result of large dihedral angle between carbazole and phenothiazine, the material inherited high thermal stability and aggregation free solid film. Also, the reasonably high HOMO (-5.37 eV) energy level suggests that incorporation of electron rich phenothiazine onto carbazole would be beneficial to increase the hole mobility. Though the structure-property relationships of fluorene, pyrene, triphenylamine, and carbazole functionalized carbazoles were well documented in the literature[5,9-13] systematic studies on structure-function correlation for carbazole-phenothiazine conjugates remained unexplored. We envisaged that introduction of non-planar phenothiazine as an end-capping unit into carbazole building block with different liking topology would be beneficial to improve the functional properties such as thermal stability, inhibition toward formation of molecular aggregates in solid film, amorphous nature and charge carrier mobility.

Halogenation of aromatics and heteroaromatics and metal catalyzed cross coupling reactions (Suzuki, Stille, Sonogashira, Buchwald-Hartwig, etc.) are the two fundamental protocols often used to access library of functional materials. Carbazole can be easily functionalized on 1, 2, 3, 6, 7 and N positions. Though the vast amount of carbazole-based materials are derived from tri-functionalization (2,7 & N or 3,6,&N), few compounds

containing chromophores on 1,8 positions are also known.[15-22] However, tri- (1,3,6) and tetra-substituted (1,3,6,8 & 2,3,6,7) derivatives are less explored. In this report, we describe carbazole-phenothiazine conjugates representing different number of phenothiazine loading on the carbazole nucleus. Di-, tri- and tetra-substituted carbazole derivatives (Chart 1) were synthesized to study the effect of thienyl-phenothiazine chromophore loading on carbazole nucleus on photophysical, electrochemical and thermal properties. To understand the electronic properties of the compounds time-dependent density functional theory (TDDFT) computations were also performed. Introduction of phenothiazine as an end-capping unit improved thermal stability of the materials significantly and led to rich redox characteristics. The electroluminescent characteristics were evaluated in multilayered OLED device by employing them as cyan or green emitting dopants in CBP host.

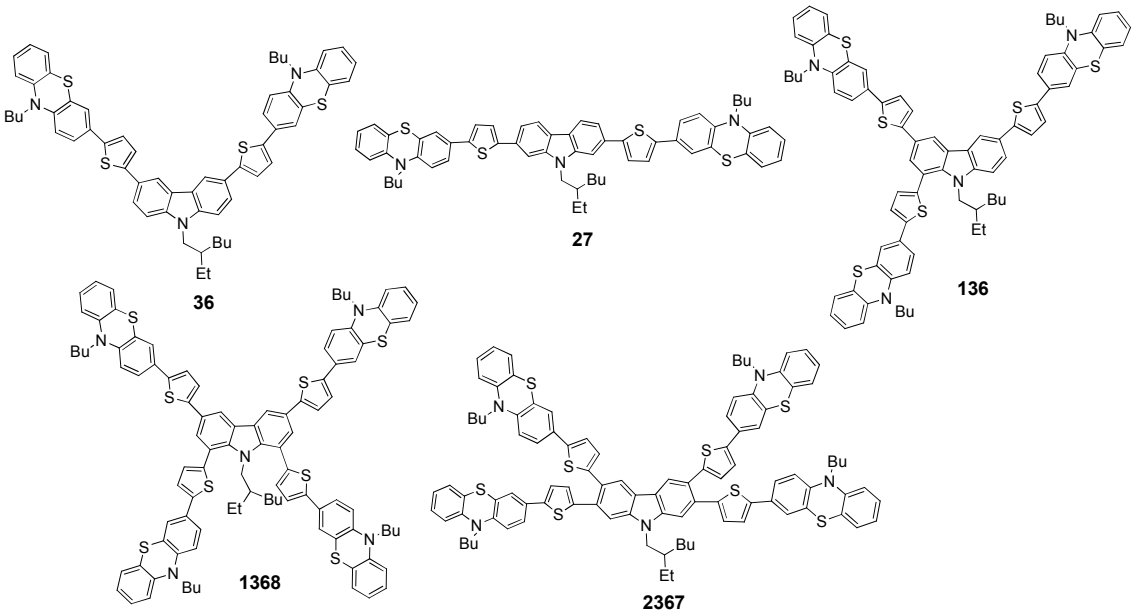

Chart 1. Structures of the compounds.

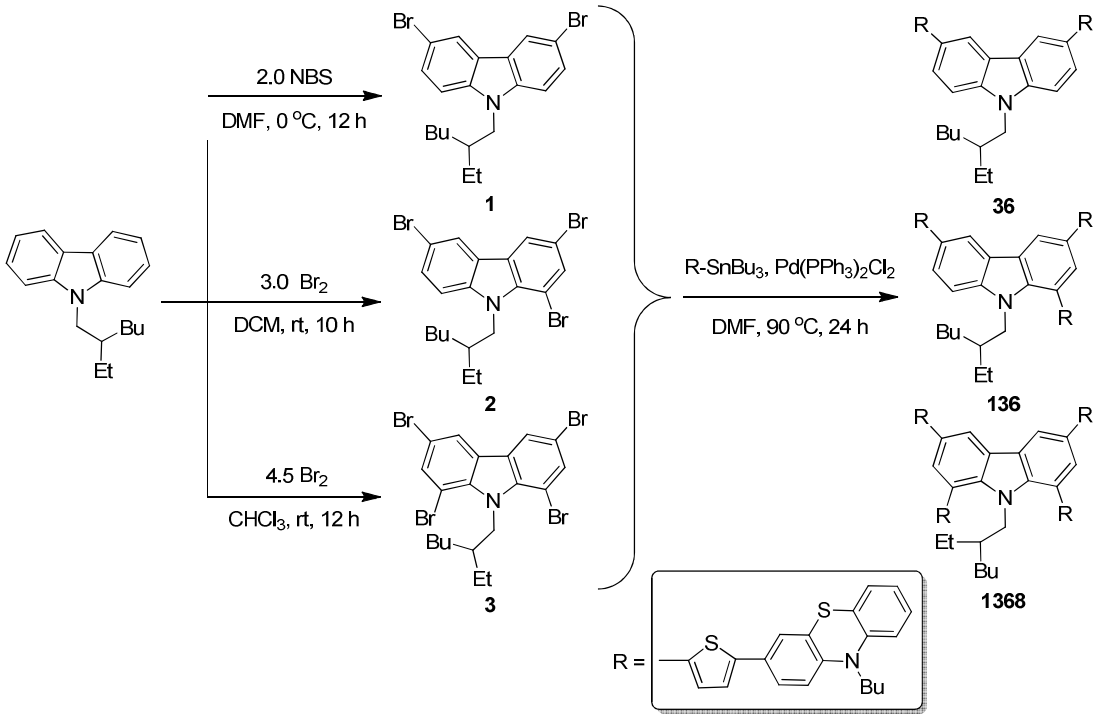

Scheme 1. Synthetic protocol for the di-(3,6), tri-(1,3,6) and tetra-(1,3,6,8)substituted derivatives.

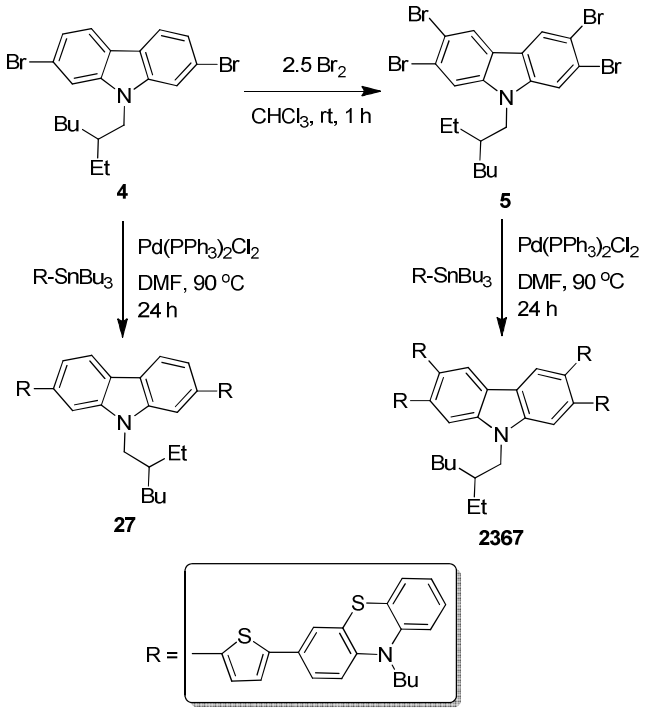

Scheme 2. Synthetic methodology for the di-(2,7) and tetra-(2,3,6,7)substituted derivatives.

RESULTS AND DISCUSSION

Synthesis and Characterization

Synthesis of the di-, tri- and tetra-substituted carbazole derivatives were accomplished as illustrated in Schemes 1 and 2. Bromination of 9-(2-ethyl-hexyl)-9*H*-carbazole using different 2.0, 3.0 and 4.5 equivalents of bromine in DMF, DCM or chloroform formed the 3,6-dibromo-, 1,3,6-tribromo- and 1,3,6,8-tetrabromo- derivatives **1**-**3** respectively. Similarly, reaction of 2.5 equivalents of bromine with 2,7-dibromo9-(2-ethyl-hexyl)-9*H*-carbazole (**4**) in chloroform produced 2,3,6,7-tetrabromo-9-(2-ethyl-hexyl)-9*H*-carbazole (**5**) in excellent yield. Finally, Stille coupling[29] reaction of the bromides (**1**-**5**) with 3-(5-tributylstannanyl-thiophen-2-yl)-10*H*-phenothiazine gave the targeted carbazole-phenothiazine hybrids in good yields. The dyes were thoroughly characterized by ^{1}H and ^{13}C nuclear magnetic resonance (NMR) spectroscopy and high resolution mass spectroscopy (HRMS). All the molecules inherited yellow color and are reasonably soluble in common organic solvents such as dichloromethane (DCM), toluene (TOL), chloroform ($CHCl_3$), tetrahydrofuran (THF) and *N,N*-dimethylformamide (DMF) but insoluble in alcohols.

Table 1. Optical properties of the dyes

Dye	λ_{max}, nm (ε_{max}, M^{-1} cm^{-1} $\times 10^{-3}$)[a]	λ_{em}, nm, (Φ_F)[a,b]	Stokes shift, cm^{-1}	λ_{em}[c], nm
27	415 (71.7), 311 (24.5)	518 (0.16)	4791	504
36	385 (53.5), 334 (46.6)	496 (0.12)	5813	494
136	375 (52.2), 307 (48.3)	517 (0.13)	7324	505
1368	382 (74.8), 324 (58.5)	505 (0.18)	6376	502
2367	382 (92.0), 315 (79.0)	526 (0.10)	7167	513

[a] Measured for DCM solution. [b] Absolute quantum yields determined by a calibrated integrated sphere system in DCM. [c] Measured for spin-cast film.

Photophysical properties

Optical properties of the compounds were evaluated by measuring absorption and emission spectra in dichloromethane. The absorption spectra of the dyes are displayed in Figure 1a and the pertinent data collected in Table 1.

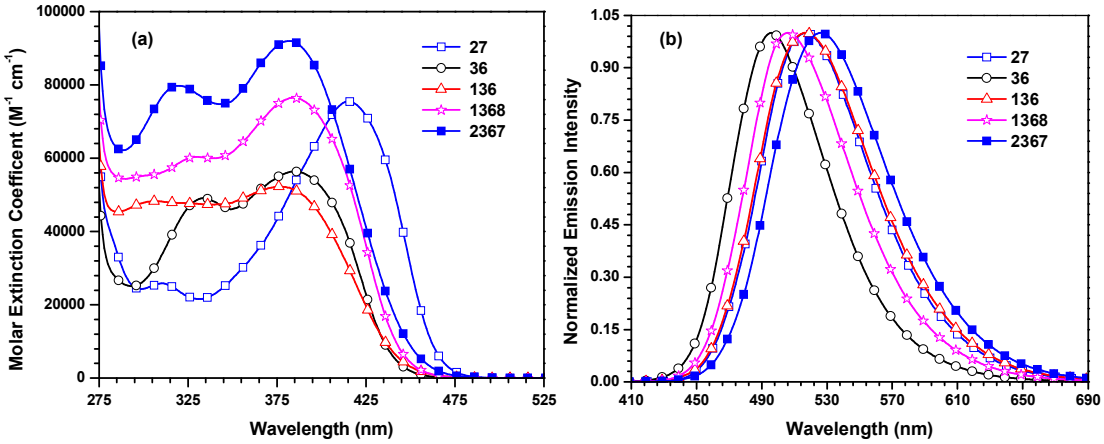

Figure 1. a) Absorption and b) emission spectra of the compounds recorded in dichloromethane.

All the dyes displayed two distinguishable absorption bands. The higher energy absorption band ca. 334-311 nm is assigned to the localized π-π* electron transitions originating from the thienylphenothiazine chromophore or carbazole core. The lower energy absorption peak ca. 382-415 nm stems from the delocalized π-π* electronic transitions from the conjugation segment comprising carbazole, thiophene and phenothiazine units. Interestingly, the dye **27** exhibited the most red-shifted absorption maxima (415 nm) in the series attributable to the higher degree of linear conjugation offered by the chromophores in the 2,7-positions of carbazole than those in 1,3,6 and 8 positions (**36**, **136** and **1368**).[9,20,30] Anomalously, the absorption spectra of **2367** is blue-shifted by 33 nm when compared to **27**. This unusual behavior is rationalized by comparing the dihedral angles between the carbazole and phenothiazine chromophores at C2 and C7 in the optimized molecules. The dihedral angle between the carbazole and thiophene units (Figure 2) is significantly larger (> 50 °) for **2367** than in **27** (25.7 °). The larger twisting would jeopardize the interchromophoric electronic communication and reduce the electronic delocalization extent. Thus, the conjugation pathway along the C2-C7 axis is perturbed in **2367** due to the additional substitution via C3 and C6. Similarly, planarity between the carbazole and thiophene units at C3 and C6 is

affected on further introduction of substituents at C2 and C7 positions (compare **36** and **2367**). On the other hand, though the substitution at C1 and C8 positions does not affect the coplanar arrangement of carbazole and thiophenes at C3 and C6 positions (compare **36**, **136**, and **1368**), the chromophores at these positions (C1 and/or C8) twisted out of the plane as a result of large dihedral angle (61.3°). Therefore the electronic communication between the chromophores at these positions (C1 and/or C8) and the central carbazole unit is not very strong in the ground state. These results suggests that the conjugation in **136** and **1368** is limited to substituents in C3 and C6**,** which resulted a similar absorption spectral profiles for these derivatives**.**[5,9,11-13] Among the tetra-substituted carbazole derivatives, **2367** exhibited intense absorption attributable to the orbital interaction of thienylphenothiazine segments at C2 and C7 via the carbazole core. Thus, dye 2367, having two thienylphenothiazine units at C2 and C7, gives a more intense absorption than dyes 1368 and 36 unsubstituted at C2 and C7. The effect of phenothiazine on the absorption spectra is evident on comparing the data observed for **27** and **36** with that of the known compounds containing thiophene only. The compounds **27** and **36** exhibited >40 nm bathochromic shift when compared to 9-ethyl-2,7-di(thiophen-2-yl)-9*H*-carbazole and 9-ethyl-3,6-di(thiophen-2-yl)-9*H*-carbazole, respectively.[8] This indicates that the end-capping by phenothiazine is beneficial for shifting the absorption to the longer wavelength region attributable to the extension of π-conjugation by phenothiazine unit.

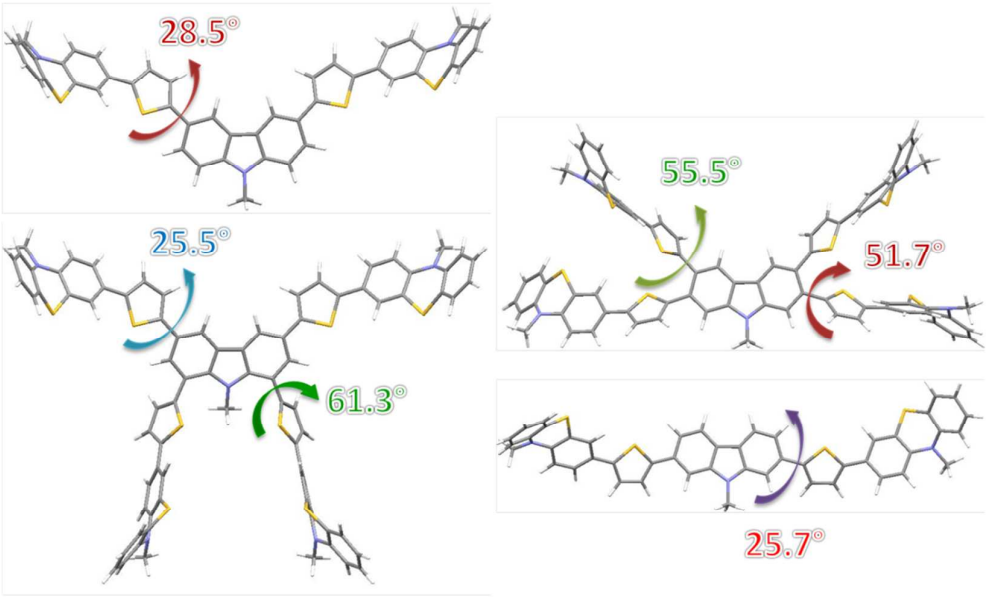

Figure 2. The variation of dihedral angles in the B3LYP/6-31G(d,p) optimized geometries of **36**, **27**, **1368** and **2367**.

It is interesting to compare the absorption profiles of **136** and **1368** with the known tri- and tetra-substituted featuring pyrene, fluorene, carbazole and triphenylamine peripheral chromophores.[5,9,11,12] Owing to the extension of conjugation by the thienylphenothiazine segments, the absorption maximum of compounds **136** and **1368** is red-shifted with respect to that of the later compounds. The absorption profiles of the dyes were examined in different solvents by varying Reichardt polarity index ($E_T(30)$)[31] *viz.*, cyclohexane (CH), toluene (TOL), tetrahydrofuran (THF), dichloromethane (DCM), chloroform ($CHCl_3$) and *N,N*-dimethylformamide (DMF). Corresponding spectra are shown in Figures (3a and **S1**-**S4)** and relevant data listed in Table **S1**. They indicate that the ground state of the dyes is relatively non-polar and devoid of significant solvent effects.

The dyes are emitting in cyan to green region on exposure to the visible light with featureless fluorescence spectra as shown in Figure 1b. The relevant data are collected in Table 1. In contrast to the absorption trend, the emission maximum is shifted to longer wavelengths in the order, **2367** > **27** > **136** > **1368** > **36**, suggesting a redistribution of

electron density in the excited state. The dye **2367** exhibits the most red-shifted emission profile when compared to its congeners. This could be due to the efficient interaction of 3,6-arms with the central carbazole at the excited state. It is speculated that the molecules assume a more planar structure in the excited state. This is further confirmed by the large Stokes shifts observed for the dyes which fell in the range 7167-4791 cm^{-1}. Large Stokes shifts for the fluorophores generally suggest a significant structural reorganization or polarized excited state as compared to that of ground state. The higher Stokes shift for the dyes **136, 1368** and **2367** as compared to the **27** and **36** can be attributed to larger structural reorganizations in the excited state for the former compounds due to a sterically congested molecular structure. It is to be noted here that the reasonably large Stokes shifts is beneficial for their application in electroluminescent devices which may help to avoid unwanted self-absorptions.[17,32]

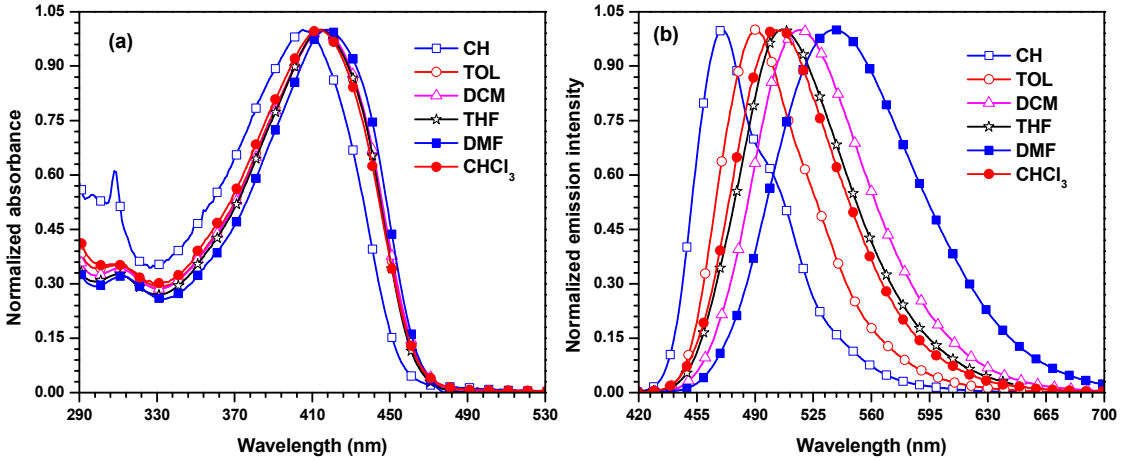

Figure 3. (a) Absorption and (b) emission spectra of the dye **27** recorded in different solvents.

In order to investigate the impact of solvent polarity on the nature of exited state of the dyes, emission profiles (Figure 3b and **S1-S4**) of the dyes were examined in solvents with different Reichardt polarity index ($E_T(30)$). The emission characteristics are highly sensitive to the solvent polarity, exhibiting a general positive solvatochromism. For instance, emission spectra recorded for the dye **27** in different solvents is displayed in Figure 3b. The moderate emission shift witnessed for the dyes on moving from CH to DMF is interesting. As the dyes

do not possess a trivial donor-acceptor molecular configuration the observed solvent induced emission wavelength shift cannot be rationalized by considering charge-transfer excitation. It is probable that the structural reorganization for the dyes induced by photo-excitation is appreciable. Particularly, the molecular structural perturbations are more pronounced in polar solvents. It is also arguable that the excitation induced dipole of the molecules is stabilized by interaction with the solvent dipoles. It has been observed in selected systems the incorporation of electron rich chromophore on C2 and C7 of carbazole induces push-pull architecture due to the difference in electron-density between the chromophores.[33] Among the dyes, **2367** exhibited significant solvent induced alternations in the emission spectra ($\Delta\lambda$ = 75 nm). The difference in Stokes shift for the compounds between the non-polar (CH) and polar solvent (DMF) can be considered as the estimate of charge transfer character in dipolar compounds.[34] This assumes the following order: **2367** > **27** > **1368** > **136** > **36** and suggests decent charge migration in the excited state for the compounds bearing substitutions in C2 and C7.

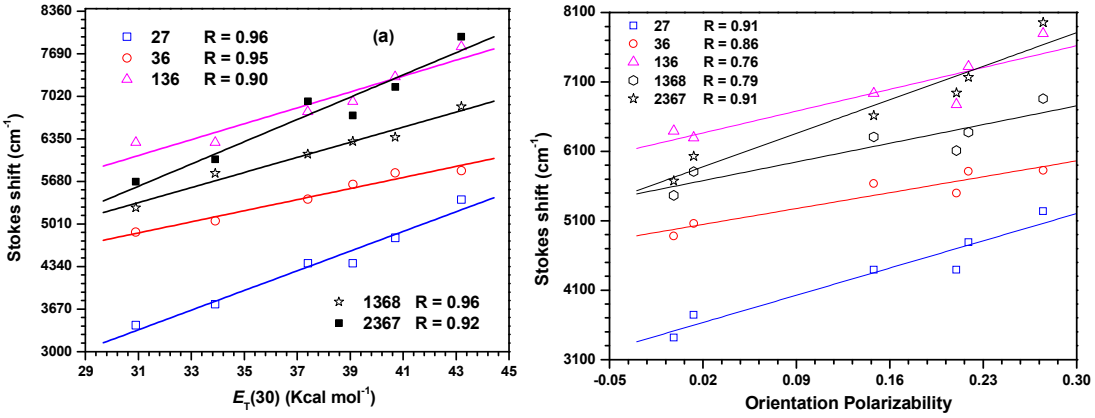

Figure 4. (a) Stokes shift vs $E_T(30)$ and (b) Lippert-Mataga plots for the dyes

The solvatochromic data of the dyes were also examined by Lippert-Mataga and Stokes shift versus $E_T(30)$ correlations. A linear trend (Figure 4) observed for the dyes indicate a general solvent effect for them in the excited state. The change ($\Delta\mu = \mu_e - \mu_g$) in dipole moment, estimated from the plots,[35,36] is more positive (Table 2) and suggestive of a large

dipole moment for the molecules in the excited state. This is a favorable condition for the presence of weak charge transfer in these molecules. Among the dyes, **27** and **2367** exhibit a large change in dipole moment (Δμ) confirming the more pronounced ICT for these molecules in the excited state. The quantum yield of the dyes decreases on increasing the solvent polarity (Table **S2**), which is suggestive of charge transfer excited state in these molecules. Also, the emission profile broadened on moving from non-polar CH to the polar DMF. This probably supports the speculation that the initially formed Frank-Condon state or local excited state transforms into the more polar charge transfer state which is stabilized by the polar solvents.[35]

Table 2. Excited and ground state dipole moments calculated in different methods[35,36]

Dye	μ_g, (D)[a]	μ_e, (D)			
		Lippert-Mataga	Reichardt	Kawski	ν_{max} *vs* Δf
27	5.61	38.66	22.80	16.71	39.04
36	3.20	23.26	13.61	7.38	26.24
136	3.95	28.10	16.57	10.41	30.55
1368	5.24	27.91	17.70	12.60	30.74
2367	2.30	37.45	19.85	12.77	38.29

[a] Estimated from the B3LYP/6-31G(d,p) calculations.

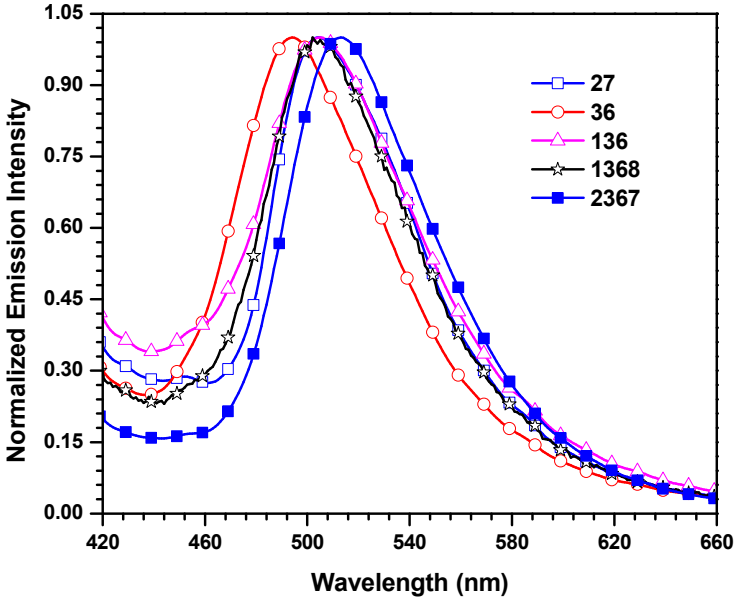

Figure 5. Emission spectra of the drop-cast thin films of the dyes.

The emission spectra of the dyes recorded as the drop-cast thin film are displayed in Figure 5. The emission maxima of the dyes match with those observed for the tetrahydrofuran solutions (Table 1). This indicates that the dielectric constants of the thin films are close to that to that of tetrahydrofuran solutions. Absence of anomalous red-shifted emission peak/shoulder for these compounds show the beneficial role of butterfly shaped phenothiazine chromophore in retarding the formation of molecular aggregates in the solid state.

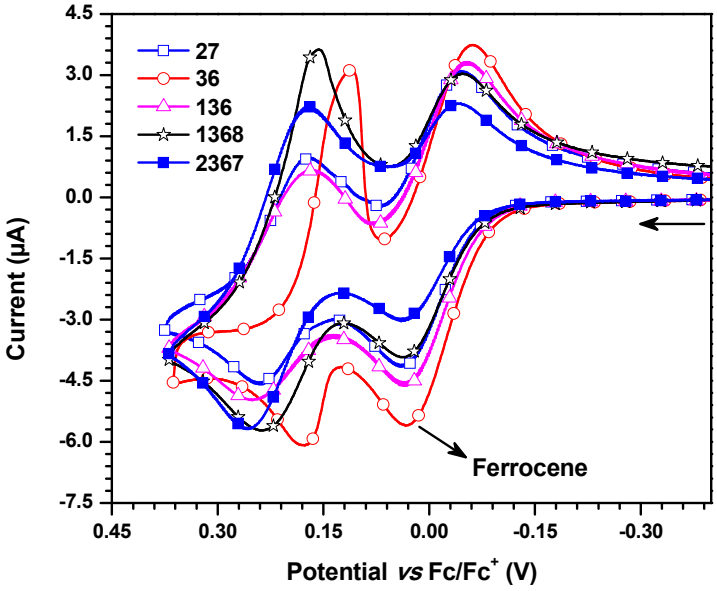

Figure 6. Cyclic voltammograms recorded for the dyes in dichloromethane (conditions, ~1×10^{-4} M solutions; scan rate 100 mV/s; electrolyte, tetrabutylammonium perchlorate)

Electrochemical properties

To ascertain the redox propensity of the dyes, cyclic voltammetric measurements were performed for the dyes in dichloromethane. The representative cyclic voltammograms recorded at a 100 mV/s scan rate are displayed in Figure 6 and the relevant data collected in Table 3. All dyes exhibited a quasi-reversible oxidation process at more positive potentials than that observed for ferrocene under the same conditions, attributable to the removal of

electron from the thienylphenothiazine arm. Generally, the dyes possess low oxidation potentials attesting the electron-richness of the phenothiazine unit. The auxiliary effect of carbazole on the phenothiazine oxidation capability is understandable on comparing the different positional substitutions. The dye-containing 3,6-disubstitution (**36**) exhibited the lowest oxidation potential among the compounds. It points to the effective conjugation between the carbazole nitrogen and the thienylphenothiazine arms through C3 and C6 positions. But, introduction of additional groups at C1 and C8 or C2 and C7 positions led to the increment in oxidation potential. The increase is more for C2 and C7 substitution (**2367**). This suggests the molecular twisting due to the additional chromophore loading which affects the conjugation for C3 and C6 substitutions. Since the arms present in C2 and C7 are closer to C3 and C6, they led to more severe distortions in the structure (*see above*). Though the C2 and C7 substituted derivatives display elongated rod-like conjugation, the involvement of nitrogen electrons in the delocalization is less favored due to *meta*-like linkage with respect to nitrogen. So the 2,7-disubstituted carbazoles generally show high oxidation potentials than the analogous 3,6-disubstituted carbazoles.[8,9] Further the effect of phenothiazine end-capping on oxidation potentials of the dyes is evident on comparing the data observed for **27** and **36** with that of the thiophene substituted carbazoles.[8] The new dyes exhibited low positive oxidation potentials when compared to the thienylcarbazoles.[8] Also, it is interesting to compare the electrochemical behavior of **27** and **36** with 5,5'-bis(10-hexyl-10*H*-phenothiazin-3-yl)-2,2'-bithiophene.[26] Insertion of carbazole between the two thienyphenothiazine units of the later with different linking topology improved the oxidation propensity significantly.

The HOMO energies of the compounds were estimated by using the first oxidation potential and falls in the range 4.95-5.02 eV. The LUMO energy values were calculated by using subtracting the optical band gap ($E_{0\text{-}0}$) from HOMO energy. The $E_{0\text{-}0}$ value was determined from the intersection of absorption and emission spectra. Generally, the HOMO

and LUMO energies of the materials are sensitive to the electron donating and withdrawing segments attached to the π-electronic system, respectively. The incorporation of electron donating units normally raises the HOMO energy level. But, in the present series of compound an anomalous trend was observed. Interestingly, the HOMO of the tri- (**136**) and tetra-substituted (**1368** & **2367**) dyes is lower in energy than that of the di-substituted derivative **36**. This is mainly due to the steric crowding induced electronic deconjugation in the molecule. Similar observations have been made earlier for 1,3,6,8- and 1,3,6-substituted carbazole derivatives.[5,9,11-13]

Table 3. Thermal and Electrochemical data of the dyes

Dye	T_{onset}, °C[a]	T_d, °C	T_m, °C	E_{ox}, V (ΔE_p, mV)[b]	HOMO, eV[c]	LUMO, eV[d]	$E_{0\text{-}0}$, eV[e]
27	385	463	190	0.21 (61)	-5.01	-2.30	-2.71
36	390	464	140	0.15 (59)	-4.95	-2.11	-2.84
136	392	472	150	0.22 (70)	-5.02	-2.23	-2.79
1368	400	480	170	0.19 (60)	-4.99	-2.19	-2.80
2367	398	478	230	0.22 (70)	-5.02	-2.32	-2.70

[a] Temperature corresponding to 10% weight loss. [b] Measured for 0.1M dichloromethane solutions and the potentials are quoted with reference to ferrocene internal standard. [c] HOMO = 4.8 + E_{ox}. [d] LUMO = HOMO-$E_{0\text{-}0}$. [e] Optical band gap obtained from the intersection of normalized absorption and emission spectra.

Thermal properties

Thermal stability of the compounds was examined by thermogravimetric analysis (TGA) under N_2 atmosphere at a heating rate of 10 °C/min. All dyes exhibited excellent thermal stability with high thermal decomposition temperature (T_d) in the range 463-478 °C. The onset decomposition temperatures corresponding to the 10% weight loss (T_{onset}) are in the range 385-400 °C. The tetra-substituted derivatives (**1368** and **2367**) are markedly more thermally stable than the di- (**36** and 27) and tri-substituted (**136**) analogs. It is noteworthy that the thermal stability of **136** and **1368** is much better than that of tetra- substituted carbazole-fluorene[9] and comparable to that of the carbazole-pyrene and carbazole-

triphenylamine conjugates.[5,12] This suggests that the phenothiazine group is helpful to improve the thermal robustness of the molecules.

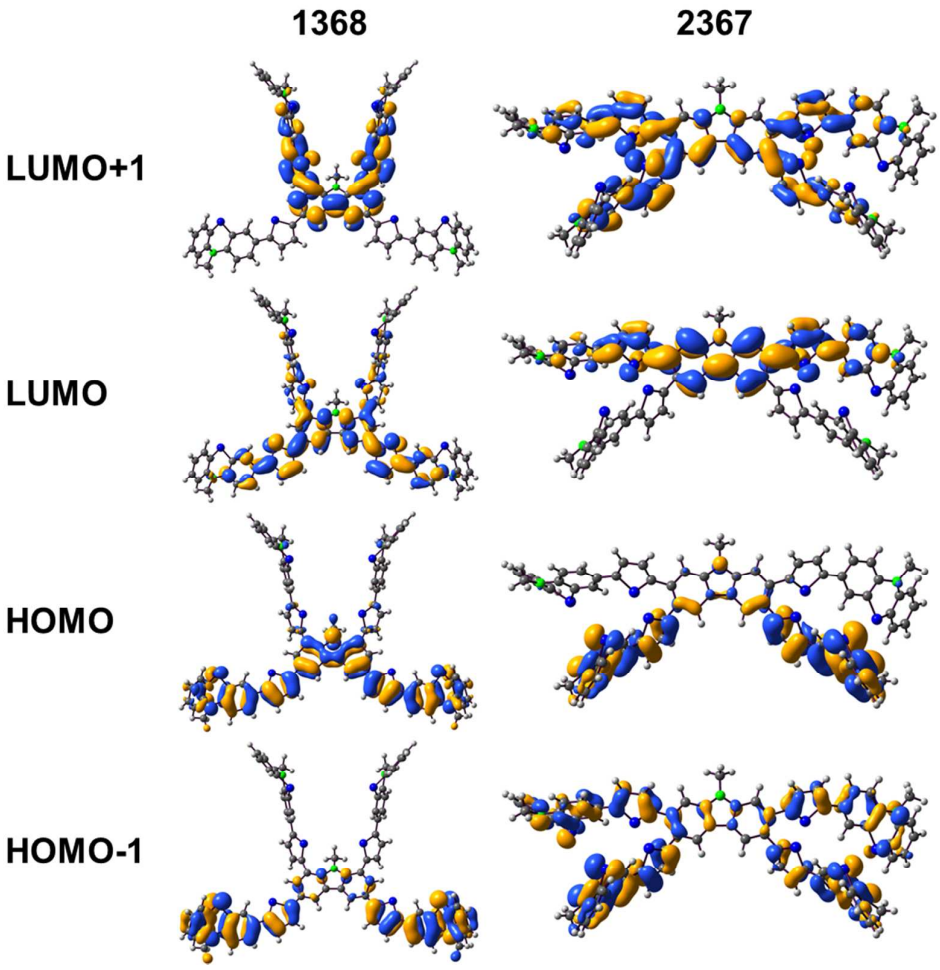

Figure 7. Frontier molecular orbitals (HOMO and LUMO) for the model compounds of **2367** and **1368** computed at the B3LYP/6-31G(d) level.

Theoretical studies

To establish a correlation between the photophysical behavior and geometry of these materials, we have performed theoretical calculations using density functional theoretical methods.[37] To minimize the computational cost, lengthy alkyl chains were replaced with the methyl segment in the model compounds. We presumed that the replacement of alkyl chains would not affect the parameters required for the discussion here. The geometries of the model compounds were optimized under vacuum by using density functional theory (DFT) with the

Becke's three parameter functional that was hybridized with the Lee-Yang-Parr correlation functional and 6-31 G(d,p) basis set.[38] TDDFT computations at the same theoretical level were used to estimate the vertical excitations and their orbital contributions.

The electronic distribution in the frontier molecular orbitals of the tetra-substituted derivatives **1368** and **2367** are shown in Figures 7 and **S5**. The HOMO is mainly contributed by the thienylphenothiazine arms in the C3 and C6 in the dyes **36**, **136**, **1368** and **2367**. It is diffused into the central core except for **2367**. The deconjugation of central carbazole from the thienylphenothiazine arms in C3 and C6 for **2367** is mainly caused by the steric crowding due to the substitution at C2 and C7. In **27**, the HOMO is delocalized over the entire molecule. The LUMO in the molecules are invariably constituted by the carbazole core and the thiophene linker for all the dyes except **2367**. In case of **2367**, the LUMO is spread over the carbazole and thiophene segments at 2,7-positions. The well separated arrangement of HOMO and LUMO in **2367** is indicative of charge transfer excited state for the HOMO to LUMO electronic transition. This may be also beneficial for the bipolar charge transport retards the reverse energy transfer in electroluminescent devices.[17,28] HOMO-1 is restricted to the thienylphenothiazine arms in C2, C3, C6 and C7. Interestingly, the thienylphenothiazine arms in C1 and C8 did not contribute to the formation of HOMO-1. However, the LUMO+1 for the dyes **136** and **1368** are predominantly composed by the arms attached to the C1 and C8 while for the remaining compounds it is mainly on the thiophene linker. These results reveal that the substitution at C1 and/or C8 may be utilized to fine-tune the electron-accepting ability of the molecules. The energies of the HOMO and LUMO levels, HOMO-LUMO energy gap values computed for the dyes (**27**, **36**, **136**, **1368** and **2367**) are listed in Table S3. The computed HOMO and LUMO energy levels fall in the narrow range of 4.70-4.79 eV and 1.19-1.54 eV, respectively. The band gap (HOMO-LUMO) of the dyes is in the range of 3.23-3.55 eV. The LUMO energies and the energy gap calculated for the dyes in the gas

phase significantly deviated from the values deduced from electrochemical and optical measurements respectively, which probably indicate a role of solvent interaction with the molecules.

The computed energies of the vertical excitations and their oscillator strengths and orbital contributions are listed in the Table **S3**. The calculated lowest energy vertical transition for the compounds in vacuum phase is in agreement with the experimentally observed results for the dyes in dichloromethane solution. This observation further supports the absence of significant solvent polarity effect on the ground state which corroborates the solvent insensitive absorption spectra recorded for the compounds.

Table 4. Computed reorganization energies for hole (λ_+) and electron (λ_-), ionization potentials (I_p) and electron affinities (E_a) (all values are in eV) for optimized models of dyes

Dye	I_p^a	I_p^v	E_a^a	E_a^v	λ_+	λ_-
36	5.47	5.60	0.79	0.61	0.24	0.34
27	5.45	5.57	0.50	0.29	0.23	0.35
136	5.38	5.48	0.60	0.43	0.19	0.27
1368	5.32	5.40	0.64	0.49	0.16	0.24
2367	5.36	5.44	0.77	0.55	0.15	0.36

In order to evaluate the charge carrier mobility (hole and electron) of these materials, internal reorganization energies for the electron (λ_-) and hole (λ_+) were calculated theoretically at the B3LYP/6-31G(d,p) level. According to Marcus-Hush equation,[39] charge transfer rate mainly depends on the two key parameters such as reorganization energy ($\lambda_{h/e}$) and electronic coupling matrix (V).

$$\mathrm{K_{hole/electron}} = \left[\frac{4\pi^2}{\mathrm{h}}\right] \frac{1}{\sqrt{4\pi \mathrm{K_B} T \lambda_{+/-}}} V^2 exp\left[-\frac{\lambda_{+/-}}{4\mathrm{K_B}T}\right]$$

Experimentally, V values are in the narrow range and it is tedious to determine the accurate V value in amorphous solid films because of direct contact.[40] However, charge mobility can be directly correlated with the respective reorganization energies ($\lambda_{+/-}$) of the materials and it is

inversely proportional to the charge transfer rate. Using this relation, reasonable correlation between the molecular structure and charge transfer rate in organic semiconductors have been established.[41] The calculated internal reorganization energies ($\lambda_{+/-}$) of the materials are listed in Table 4. As mentioned above, small $\lambda_{+/-}$ indicates larger charge mobility. The hole reorganization energies (λ_{+}) decrease with increasing the phenothiazine chromophore loading on carbazole. Thus, the tetra-substituted compounds **1368** and **2367** are predicted to possess high hole mobility in the series. The ionization potentials of the compounds were in agreement with the above trend. The electron reorganization energies (λ_{-}) of the compounds are slightly larger indicating poor electron mobility in the molecular layers.

Electroluminescence Characteristics

The electroluminescence of the compounds was examined by using them as emitting dopants in solution processed multilayered OLED devices. The device configuration is ITO/PEDOT:PSS/CBP+**36** or **27** or **136** or **1368** or **2367** (10 wt%)/TPBI/LiF/Al, where poly(3,4-ethylene-dioxythiophene)-poly-(styrenesulfonate) (PEDOT:PSS) served as hole transporting layer (HTM) while 1,3,5-tris(N-phenylbenzimidazol-2-yl)benzene (TPBi) functioned as electron-transport material (ETM). The organic layers were sandwiched between the ITO anode and Al cathode. An additional electron injection layer (LiF) was also used. For the doped devices, 4,4'-bis(9H-carbazol-9-yl)biphenyl (CBP) was used as host material. The energy level alignment for the materials used in the devices is depicted in Figure 8. From this it is understandable that the hole injection barrier at the HTM/dye interface is small (<0.1 eV) and favorable for effective hole injection. However, there is significant barrier (<0.38 eV) for electron injection from the ETM into the dyes. This may relatively hinder the electron flow into the dye layer. Interestingly, the dyes containing substitution at C2 and C7 (**27** and **2367**) possess relatively less barrier for electron injection.

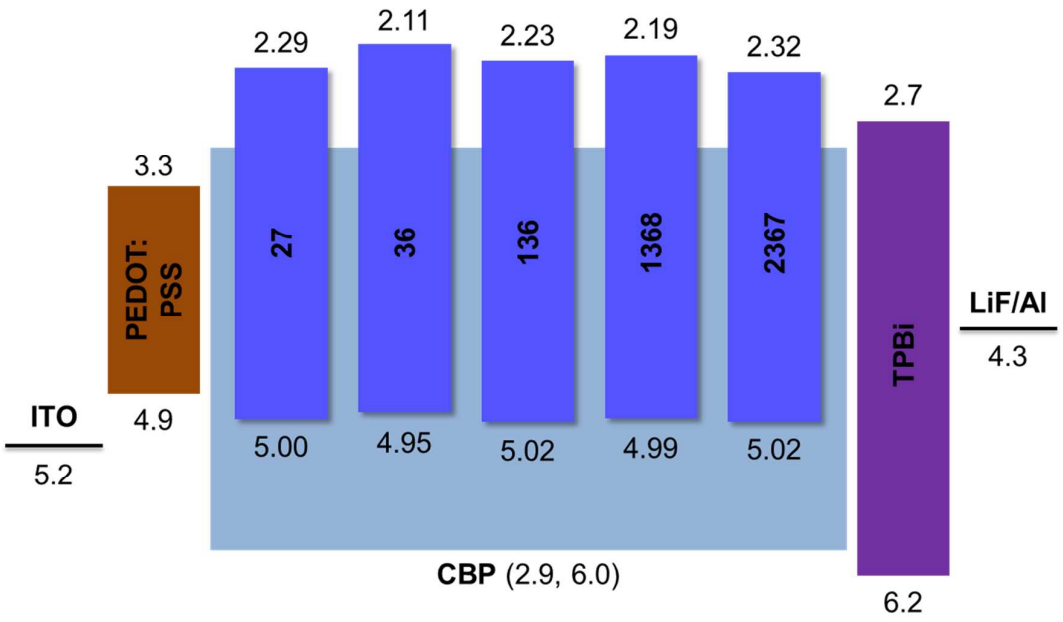

Figure 8. Energy level diagram of the OLED device that were doped with 10 wt% of **27**, **36**, **136**, **1368** and **2367** (All values are in eV with respect to vacuum level).

The current-density vs voltage (*I-V*), current-density vs luminance plots (*I-L*) of the doped OLED devices are shown in Figure 9 and the pertinent electroluminescence parameters listed in Table 5. The dyes containing substitution at C2 and C7 (**2367** and **27**) exhibited relatively low turn-on voltages (V_{on}) attributable to the low lying LUMO energy level. This would facilitate the effective injection of electrons in the corresponding molecular layers. Also they exhibited reasonably high luminance reflecting their emission characteristics and effective exciton capture from the host matrix. In electroluminescence (EL) spectra (Figure 10), the bright green emission was observed for the devices (**27**, **136** and **2367**) with the peaks centered at (500-508 nm) and Commission International de l'Éclairage coordinates (CIE) ((0.23, 0.54), (0.21, 0.46) and (0.23, 0.54)). For the devices doped with **1368** and **36**, cyan emission was observed at the wavelength maxima of 484 nm and 492 nm, respectively with CIE coordinates of 0.17, 0.35 and 0.19, 0.39. The EL spectra of the diodes resemble the photoluminescence (PL) spectra of the materials as thin film. These results further confirmed

that the obtained electroluminescence from the doped devices is from the desired emitting layer (EML) and lack of aggregate formation in the solid state. Also, the observed EL spectra of the OLED persisted over the entire operating voltages studied. The narrow FWHM values of the electroluminescence spectra indicate the color purity of the devices. Overall, the best performance was observed for **2367** doped device with maximum luminescence and current efficiency. This may attributed to the efficient trapping of excitons by **2367** from CBP layer owing to the favorable alignment of energy levels with the host matrix.

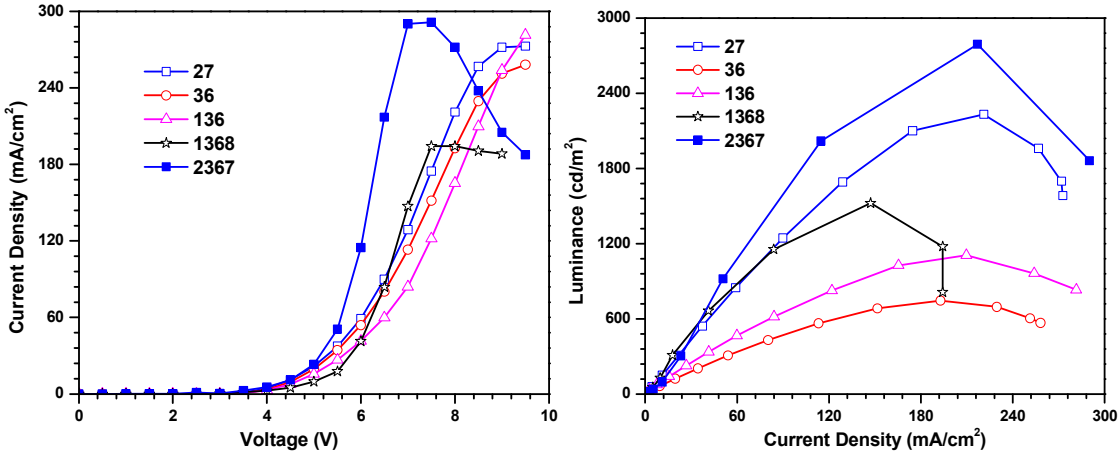

Figure 9. *I-V-L* characteristics of the OLEDs doped (10%) with **27**, **36**, **136**, **1368** and **2367**.

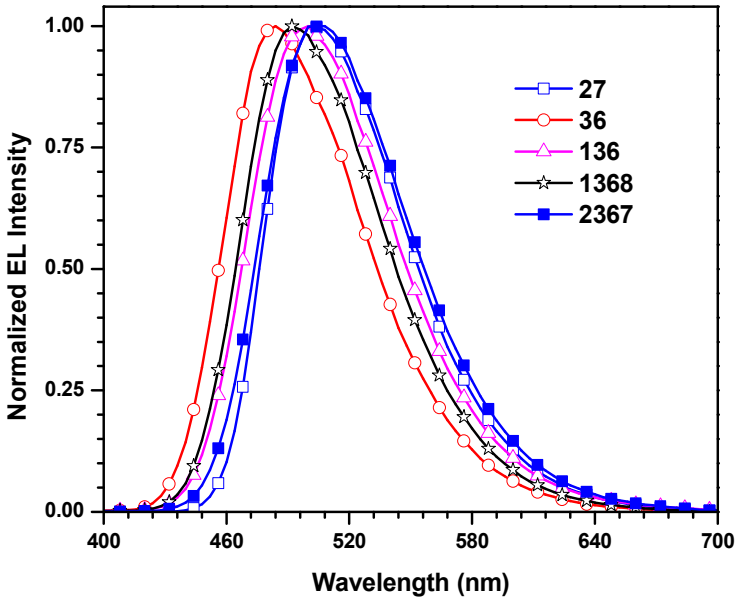

Figure 10. The electroluminescence spectra of the doped (10%) of **27**, **36**, **136**, **1368** or **2367**.

Table 5. Device performance characteristics of the doped (10%) OLEDs.

Dye	V_{on}, V[a]	η_c, cd/A[b,c]	L_{max}, cd/m^2	λ_{EL}, nm	FWHM, nm	CIE (x,y)[c]
27	4.2	1.3/1.4	2233	500	81	(0.23,0.54)/(0.23,0.53)
36	4.8	0.6/-	754	484	75	(0.17,0.35)/-
136	4.7	1.0/0.6	1107	500	80	(0.21,0.46)/-
1368	4.8	1.2/1.4	1523	492	78	(0.19,0.39)/(0.19,0.42)
2367	4.5	0.9/1.8	2791	508	84	(0.23,0.52)/(0.23,0.51)

[a] turn-on voltage. [b] current efficiency. [c] at 100/1000 cd/m^2

CONCLUSIONS

In summary, we have synthesized a new class of polysubstituted carbazoles with phenothiazine chromophore linked via a thiophene spacer as cyan or green emitters in solution processed doped OLED. The absorption spectra of the compounds are highly dependent on the substitution pattern and are insensitive to the solvent polarity. But, the emission spectra were significantly altered by the polarity of solvent and the observed positive solvatochromic behavior suggest a more polar excited state involving significant structural changes. The emission characteristics such as large Stokes shift, featureless broad fluorescence and large dipole moment change support the structural change in the excited molecule involving electronic redistribution. Lippert-Mattga and $E_T(30)$ correlations of the solvatochromic data and DFT calculation results suggest a more polar excited state for the molecules **2367** and **27** than their congeners. The tetra-substituted derivatives displayed high thermal stability in the series. Solution processed multilayered OLED were fabricated by employing **27**, **36**, **136**, **1368** and **2367** as dopants in CBP host matrix and found to exhibit bluish green emission. A device fabricated with **2367** exhibited superior performance in the series attributable to the well aligned energy levels and emission characteristics. Further studies to exploit the use of these materials as hole transporting materials in photovoltaic devices are under progress in our laboratory.

EXPERIMENTAL SECTION

General Methods

All required precursor chemicals were obtained from commercial sources used as received without any further purification. The solvents used for synthesis and analytical measurements were dried by following standard procedures and distilled prior to use. Column chromatography technique was performed on 100-200 mesh silica as the stationary phase in a 30 cm long and 2.0 cm diameter column. ^{1}H and ^{13}C NMR spectral data were collected in $CDCl_3$ on FT-NMR spectrometer operating at 500.13 and 125.77 or 400 and 100.00 MHz, respectively. Me_4Si (0.00 ppm) was used as internal standard to calibrate the chemical shift values. Mass spectral (HRMS) data were recorded on ESI TOF high resolution mass spectrometer in positive mode. The electronic absorption and emission spectral data were collected at room temperature using a UV-vis spectrophotometer. Appropriate dilute solutions were used for the measurements which were performed at room temperature. Absolute quantum yield were determined by a calibrated integrating sphere connected to the spectrofluorimeter. Cyclic voltammetry experiments were performed by using an electrochemical analyzer with a conventional three-electrode configuration consisting of a glassy carbon working electrode, platinum auxiliary electrode, and a non-aqueous $Ag/AgNO_3$ reference electrode. The $E_{1/2}$ values were determined as $(E_p^a+E_p^c)/2$, where E_p^a and E_p^c are the anodic and cathodic peak potentials, respectively. The potentials are quoted against ferrocene internal standard. Thermogravimetric analysis (TGA) was performed under nitrogen atmosphere at heating rate of 10 °C /min.

SYNTHESIS

The precursors **1** and **4** was synthesized according to the following literature procedure.[42]

1,3,6-Tribromo-9-(2-ethyl-hexyl)-9*H*-carbazole (2).

To a stirred solution of 9-(2-ethyl-hexyl)-9*H*-carbazole (1.00 g, 7.15 mmol) in 20 mL of dichloromethane in a 250 mL round bottom flask, bromine (1.10 mL, 22.16 mmol) diluted in 10 mL dichloromethane was added drop wise through a dropping funnel at room temperature for 10 min. After the addition, stirring was allowed for further 10 h at room temperature. After completion of reaction, excess of bromine was removed by washing with aqueous sodium hydrogen sulfate. The reaction mixture was extracted with DCM (2 × 20 mL), dried over anhydrous sodium sulfate and evaporated to dryness. The resultant crude product was purified by column chromatography using hexanes as eluent to offer the title compound **2** (1.36 g, 60%) as white color solid; mp 120-130 °C; ^{1}H NMR (500.13 MHz, $CDCl_3$, δ ppm): 8.02 (d, J = 5.0 Hz, 1H), 7.97 (d, J = 1.5 Hz, 1H), 7.69 (d, J = 2.0 Hz, 1H), 7.54-7.52 (m, 1H), 7.21 (d, J = 9.0 Hz, 1H), 4.45-4.33 (m, 2H), 2.05-2.00 (m, 1H), 1.32-1.12 (m, 8H), 0.81 (t, J = 7.0 Hz, 6H); ^{13}C NMR ($CDCl_3$, 100.00 MHz, δ ppm): 140.7, 135.9, 133.6, 129.5, 126.1, 122.8, 122.0, 112.6, 111.7, 103.5, 48.0, 40.4, 30.2, 28.4, 23.5, 23.0, 13.9, 10.8; HRMS calcd for $C_{20}H_{22}NBr_3$ $[M+H]^+$ m/z 514.9282, found 514.9283.

1,3,6,8-Tetrabromo-9-(2-ethylhexyl)-9H-carbazole (3).

It was obtained from carbazole (1.5 g, 5.37 mmol) and bromine (1.7 mL, 26.85 mmol) by following the procedure described above for **2**, but chloroform was used as solvent. White crystalline solid; Yield: 2.4 g, 76%; mp 130-140 °C; ^{1}H NMR (500.13 MHz, $CDCl_3$, δ ppm): 8.05 (d, J = 2 Hz, 2H), 7.77 (d, J = 1.5 Hz, 2H), 5.13 (d, J = 8 Hz, 2H), 1.85-1.81 (m, 1H), 1.10-1.00 (m, 8H), 0.74-0.69 (m, 6H); ^{13}C NMR ($CDCl_3$, 100.00 MHz, δ ppm): 134.8, 121.9, 112.9, 105.1, 48.3, 40.0, 29.0, 27.7, 22.9, 22.2, 13.0, 10.4; HRMS calcd for $C_{20}H_{21}NBr_4$ $[M+H]^+$ m/z 594.8366, found 594.8367.

2,3,6,7-Tetrabromo-9-(2-ethyl-hexyl)-9*H*-carbazole (5).

It was obtained from 2,7-dibromo-9-(2-ethyl-hexyl)-9*H*-carbazole (2.0 g, 4.50 mmol) and bromine (1.0 mL, 11.25 mmol) by following the procedure described above for **2**, but

chloroform was used as solvent. In the final step, a white precipitate was obtained which was found to be analytically pure enough and so no column chromatography was required. Yield: 2.15 g, 96%; mp 118-125 °C ^{1}H NMR (500.13 MHz, $CDCl_3$, δ ppm): 8.21 (s, 2H), 7.62 (s, 2H), 4.01 (t, J = 10.0 Hz, 2H), 1.99-1.94 (m, 1H), 1.36-1.24 (m, 8H), 0.92-0.87 (m, 6H); ^{13}C NMR ($CDCl_3$, 100.00 MHz, δ ppm): 140.7, 124.7, 122.2, 122.0, 114.6, 114.0, 47.8, 39.0, 30.7, 28.4, 24.2, 22.9, 14.0, 10.8; HRMS calcd for $C_{20}H_{21}NBr_4$ $[M+H]^+$ m/z 594.8366, found 594.8367.

3,3'-(5,5'-(9-(2-Ethylhexyl)-9*H*-carbazole-3,6-diyl)bis(thiophene-5,2-diyl))bis(10-butyl-10*H*-phenothiazine) (36). A mixture of **1** (0.70 g, 1.62 mmol), 10-butyl-3-(5-tributylstannanyl-thiophen-2-yl)-10*H*-phenothiazine (2.60 g, 4.00 mmol), $Pd(PPh_3)_2Cl_2$ (1 mol%) were dissolved in 10 mL of DMF and degassed with N_2 for 15 min in a 100 mL round bottom flask. The reaction mixture was heated at 90 °C for 24 h under N_2 atmosphere. After completion of reaction, distilled water (40 mL) was added and extracted with DCM, dried over anhydrous sodium sulfate and dried. The resultant crude product was purified by column chromatography using CH_2Cl_2:hexanes (1:3) as eluent to offer the desired compound **36** (0.72 g, 74%) as yellow color solid; mp 180-190 °C; ^{1}H NMR (500.13 MHz, $CDCl_3$, δ ppm): 8.33 (d, J = 1.5 Hz, 2H), 7.74 (dd, J = 1.5, 5.0 Hz, 2H), 7.43-7.42 (m, 4H), 7.37 (d, J = 8.0 Hz, 2H), 7.30 (d, J = 3.5 Hz, 2H), 7.20 (d, J = 3.5 Hz, 2H), 7.17-7.15 (m, 4H), 6.94-6.85 (m, 6H), 4.17-4.12 (m, 2H), 3.87 (t, J = 6.5 Hz, 4H), 2.07-2.04 (m, 1H), 1.83-1.79 (m, 4H), 1.52-1.27 (m, 9H), 0.98-0.86 (m, 15H); ^{13}C NMR ($CDCl_3$, 125.77 MHz, δ ppm): 140.8, 127.3, 125.8, 124.5, 124.0, 123.1, 122.9, 122.5, 117. 4, 115.4, 109.4, 47.5, 39.5, 31.7, 31.0, 28.8, 27.0, 24.4, 23.1, 22.7, 20.2, 14.2 13.9, 11.0; HRMS calcd for $C_{60}H_{59}N_3S_4Na$ $[M+Na]^+$ m/z 972.3489, found 972.3480.

3,3'-(5,5'-(9-(2-Ethylhexyl)-9*H*-carbazole-2,7-diyl)bis(thiophene-5,2-diyl))bis(10-butyl-10*H*-phenothiazine) (27). Compound **27** was synthesized from **4** (1.00 g, 2.29 mmol) and

10-butyl-3-(5-tributylstannanyl-thiophen-2-yl)-10*H*-phenothiazine (3.80 g, 6.87 mmol) by following as similar procedure as described above for **36**. Pale yellow solid; Yield: 1.57 g, 70%; mp 130-140 °C; ^{1}H NMR (500.13 MHz, $CDCl_3$, δ ppm): 8.03 (d, J = 8.0 Hz, 2H), 7.56 (s, 2H), 7.51-7.49 (m, 2H), 7.42-7.41 (m, 4H), 7.34 (d, J = 3.5 Hz, 2H), 7.20 (d, J = 4.0 Hz, 2H), 7.16 (d, J = 7.5 Hz, 4H), 6.94-6.91 (m, 2H), 6.88-6.84 (m, 4H), 4.21-4.17 (m, 2H), 3.87 (t, J = 5.0 Hz, 4H), 2.13-2.08 (m, 1H), 1.81 (t, J = 10.0 Hz, 4H), 1.50-1.40 (m, 9H), 0.99-0.85 (m, 15H); ^{13}C NMR ($CDCl_3$, 125.77 MHz, δ ppm): 144.9, 144.5, 144.0, 142.4, 141.9, 132.0, 128.9, 127.5, 127.3, 125.3, 124.5, 124.3, 123.9, 123.2, 122.5, 122.1, 120.6, 117.3, 115.5, 115.4, 105.8, 47.2, 39.4, 31.0, 28.9, 26.9, 24.6, 23.1, 20.2, 13.9, 11.0; HRMS calcd for $C_{60}H_{59}N_3S_4Na$ $[M+Na]^+$ m/z 972.3489, found 972.3486.

3,3',3''-(5,5',5''-(9-(2-Ethylhexyl)-9*H*-carbazole-1,3,6-triyl)tris(thiophene-5,2-diyl))tris(10-butyl-10*H*-phenothiazine) (136). Compound **136** was synthesized from **2** (0.70 g, 1.36 mmol) and 10-butyl-3-(5-tributylstannanyl-thiophen-2-yl)-10*H*-phenothiazine (3.09 g, 4.76 mmol) by following the procedure described above for **36**. Dark-yellow solid; Yield: 1.04 g, 60%; mp 220-230 °C; ^{1}H NMR (400.0 MHz, $CDCl_3$, δ ppm): 8.25 (s, 1H), 7.54 (d, J = 12.0 Hz, 1H), 7.41 (d, J = 8.0 Hz, 4H), 7.28-7.27 (m, 2H), 7.17-7.06 (m, 10 Hz), 7.05 (S, 2H), 6.88-6.86 (m, 12H), 4.11 (d, J = 4.0 Hz, 6H), 3.92 (t, J = 16 Hz, 2H), 1.80 (d, J = 4 Hz, 8H), 1.50-1.44 (m, 7H), 0.98-0.93 (m, 15H), 0.66 (t, J = 8.0 Hz, 3H), 0.56 (t, J = 4.0 Hz, 3H); ^{13}C NMR ($CDCl_3$, 100.0 MHz, δ ppm): 140.7, 136.0, 133.6, 129.6, 127.9, 127.3, 126.2, 124.8, 122.8, 122.7, 122.1, 115.7, 112.6, 103.6, 48.1, 40.4, 30.2, 28.4, 23.5, 23.0, 20.1, 13.9, 13.8, 11.0; HRMS calcd for $C_{80}H_{76}N_4S_6Na$ $[M+Na]^+$ m/z 1307.4289 , found 1307.4292.

3,3',3'',3'''-(5,5',5'',5'''-(9-(2-Ethylhexyl)-9*H*-carbazole-1,3,6,8-tetrayl)tetrakis-(thiophene-5,2-diyl))tetrakis(10-butyl-10*H*-phenothiazine) (1368). Compound **1368** was prepared from **3** (0.80 g, 1.34 mmol) and 10-butyl-3-(5-tributylstannanyl-thiophen-2-yl)-10*H*-phenothiazine (4.50 g, 6.70 mmol) by following the procedure of **36**. Yellow solid;

Yield: 1.7 g, 60%; mp 165-175 °C; ^{1}H NMR (500.13 MHz, $CDCl_3$, δ ppm): 8.34 (d, J = 2.0 Hz, 2H), 7.74 (s, 2H), 7.44-7.42 (m, 8H), 7.37 (d, J = 4.0 Hz, 2H), 7.23 (d, J = 3.5 Hz, 2H), 7.16-7.14 (m, 10H), 6.94-6.86 (m, 14H), 3.88 (t, J = 7.0 Hz, 10H), 1.82-1.79 (m, 9H), 1.51-1.42 (m, 10H), 0.98-0.94 (m, 15H), 0.51 (t, J = 7.5 Hz, 4H), 0.27 (t, J = 7.0 Hz, 5H); ^{13}C NMR ($CDCl_3$, 125.77 MHz, δ ppm): 145.0, 144.9, 144.7, 144.4, 143.8, 143.1, 141.9, 141.2, 139.3, 129.0, 128.7, 128.6, 127.6, 127.5, 127.3, 127.0, 126.4, 125.4, 125.3, 125.1, 124.8, 124.5, 124.2, 123.4, 123.1, 122.5, 122.3, 120.5, 116.8, 115.5, 115.4, 115.3, 47.2, 39.0, 34.7, 31.6, 29.0, 27.3, 26.9, 25.3, 22.7, 22.5, 20.7, 20.2, 14.1, 13.9, 11.5, 9.8; HRMS calcd for $C_{100}H_{93}N_5S_8Na$ $[M+Na]^+$ m/z 1643.5128 , found 1643.5115.

3,3',3'',3'''-(5,5',5'',5'''-(9-(2-Ethylhexyl)-9*H*-carbazole-2,3,6,7-tetrayl)tetrakis-(thiophene-5,2-diyl))tetrakis(10-butyl-10*H*-phenothiazine) (2367). Compound **2367** was synthesized from **5** (1.00 g, 1.68 mmol) and 10-butyl-3-(5-tributylstannanyl-thiophen-2-yl)-10H-phenothiazine (5.40 g, 7.56 mmol) by following the method described earlier for **36**. Yellow solid; Yield: 1.6 g, 60%; mp 150-160 °C; ^{1}H NMR (500.13 MHz, $CDCl_3$, δ ppm): 8.19 (s, 2H), 7.51 (s, 2H), 7.36-7.34 (m, 8H), 7.16-7.11 (m, 8H), 7.09-7.08 (m, 4H), 6.91-6.81 (m, 16H), 4.22-4.16 (m, 2H), 3.86-3.82 (m, 8H), 2.13 (t, J = 10.0 Hz, 1H), 1.80-1.76 (m, 8H), 1.48-1.43 (m, 14H), 0.98-0.86 (m, 20H); ^{13}C NMR ($CDCl_3$, 100.00 MHz, δ ppm): 144.8, 144.4, 143.4, 140.6, 128.7, 127.9, 127.4, 127.2, 125.1, 124.8, 124.7, 124.5, 124.0, 123.9, 122.3, 122.0, 121.9, 115.3, 115.2, 114.5, 113.9, 47.5, 47.0, 38.9, 30.5, 28.8, 28.3, 24.1, 22.9, 20.0, 14.0, 13.8, 10.7; HRMS calcd for $C_{100}H_{93}N_5S_8Na$ $[M+Na]^+$ m/z 1643.5126 , found 1643.5143.

OLED fabrication and characterization

The OLED devices were fabricated on a precleaned glass substrate containing ITO (thickness: 125 nm) as anode, poly(3,4-ethylene-dioxythiophene)-poly(styrenesulfonate) (PEDOT:PSS, thickness: 35 nm) as a hole-injection layer (HIL), an emissive layer (EML),

TPBI as an electron-transport layer (ETL) (thickness: 35 nm), a LiF electron-injection layer (EIL, thickness: 0.7 nm), and an Al layer (thickness: 150 nm) as a cathode. The aqueous solution of PEDOT:PSS was spin-coated at 4000 rpm for 20 s to form a 35 nm HIL layer. The dyes **27**, **36**, **136**, **1368**, and **2367** doped in 4,4'-bis(9H-carbazol-9-yl)biphenyl (CBP) were deposited by spin-coating at 2500 rpm for 20 s and served as emissive layer. Then, the TPBI layer was deposited onto it. Finally, lithium fluoride and aluminum cathode were thermally evaporated at 1.0×10^{-5} Torr.

Acknowledgements

K.R.J.T is thankful to DST, New Delhi for financial support (Ref. No. DST/TSG/PT/2013/09). DST is also acknowledged for a FIST grant to establish ESI mass spectrometer at the department. Generous access to the instrumental facility at the Department of Chemistry and Institute Instrumentation Centre is also gratefully acknowledged. R.K.K is thankful to CSIR, New Delhi for a Research Fellowship.

Supporting Information. Copies of ^{1}H and ^{13}C NMR spectra, solvatochromic plots, and Cartesian coordinates of the optimized structures. This material is available free of charge via the internet at http://pubs.acs.org.

References

1. a) Tang, C. W.; VanSlyke, S. A. *Appl. Phys. Lett.* **1987**, *51*, 913. b) Duan, L.; Hou, L.; Lee, T. W.; Qiao, J.; Zhang, D.; Dong, G.; Wang, L; Qiu, Y. *J. Mater. Chem*. **2010**, *20*, 6392. c) Zhu, X. H.; Peng, J.; Cao, Y.; Roncali, J. *Chem. Soc. Rev*. **2011**, *40*, 3509. d) Zhu, M.; Yang, C. *Chem. Soc. Rev*. **2013**, *42*, 4963. e) Chercka, D.; Yoo, S. J.; Baumgarten, M.; Kim, J. J.; Müllen, K. *J. Mater. Chem. C* **2014**, *2*, 9083. f) Zhan, X.; Sun, N.; Wu, Z.; Tu, J.; Yuan, L.; Tang, X.; Xie, Y.; Peng, Q.; Dong, Y.; Li, Q.; Ma, D.; Li, Z. *Chem. Mater*. **2015**, *27*, 1847

2. a) Thomas, K. R. J.; Lin, J. T.; Tao, Y. T.; Ko, C. W. *J. Am. Chem. Soc*. **2001**, *123*, 9404. b) Thomas, K. R. J.; Lin, J. T.; Tao, Y. T.; Ko, C. W. *Chem. Mater*. **2002**, *14*, 1354. c) Fisher,

A. L.; Linton, K. E.; Kamtekar, K. T.; Pearson, C.; Bryce, M. R.; Petty, M. C. *Chem. Mater*. **2011**, *23*, 1640; d) Krotkus, S.; Kazlauskas, K.; Miasojedovas, A.; Gruodis, A.; Tomkeviciene, A.; Grazulevicius, J. V.; Jursenas, S. *J. Phys. Chem. C* **2012**, *116*, 7561. e) Zhang, Z.; Jiang, W.; Ban, X.; Yang, M.; Ye. S.; Bin, H.; Sun, Y. *RSC Adv*. **2015**, *5*, 29708

3) a) Thomas, K. R. J.; Velusamy, M.; Lin, J. T.; Chuen, C. H.; Tao, Y. T. *J. Mater. Chem*. **2005**, *15*, 4453. b) Lo, S. C.; Burn, P. L. *Chem. Rev*. **2007**, *107*, 1097. c) Burn, P. L.; Lo, S. C.; Samuel, D. W. *Adv. Mater*. **2007**, *19*, 1675. d) Zhao, Z.; Li, J. H.; Wang, X.; Lu, P.; Yang, Y. *J. Org. Chem*. **2009**, *74*, 383. e) Moonsin, P.; Prachumrak, N.; Namuangruk, S.; Jugsuttiwang, S.; Keawin, T.; Sudyoadsuk, T.; Promarak, V. *J. Mater. Chem. C* **2014**, *2*, 5540.

4) a) Burroughes, J. H.; Bradley, D. D. C.; Brown, A. R.; Marks, R. N.; Mackay, K.; Friend, R. H.; Burns, P. L.; Holmes, A. B. *Nature,* **1990**, *347*, 539. b) Grimsdale, A. C.; Chan, K. L.; Martin, R. E.; Jokisz, P. G.; Holmes, A. B. *Chem. Rev*. **2009**, *109*, 897. c) Gong, S.; Yang, C.; Qin, J. *Chem. Soc. Rev*. **2012**, *41*, 4797. d) Stanislovaityte, E.; Simokaitiene, J.; Raisys, S.; Attar, H. A.; Grazulevicius, J. V.; Monkman, A. P.; Jankus, V. *J. Mater. Chem. C* **2013**, *1*, 8209.

5) Kotchapradist, P.; Prachumrak, N.; Tarsang, R.; Jungsuttiwong, S.; Keawin, T.; Sudyoadsuk, T.; Promarak, V. *J. Mater. Chem. C* **2013**, *1*, 4916.

6) a) Moonsin, P.; Prachumrak, N.; Namuangruk, S.; Jungsuttiwong, S.; Keawin, T.; Sudyoadsuk , T.; Promarak, V. *Chem. Commun*. **2013**, *49*, 6388. b) Valchanov, G.; Ivanova, A.; Tadjer, A.; Chercka, D.; Baumgarten, M. *Org. Electron*. **2013**, *14*, 2727. c) Tanaka, H.; Shizu, K.; Lee, J.; Adachi, C.; *J. Phys. Chem. C* **2015**, *119*, 2948. d) Sizu, K.; Tanaka, H.; Uejima, M.; Sato, T.; Tanaka, K.; Kaji, H.; Adachi, C. *J. Phys. Chem. C* **2015**, *119*, 1291. e) Albrecht, K.; Matsuotza, K.; Fujita, K.; Yamamato, K. *Angew. Chem., Int. Ed.* **2015**, *54*, 1.

7) a) Forrest, S. R.; Thompson, M. E. *Chem. Rev*. **2007**, *107*, 923. b) Kato, S.; Shimizu, S.; Taguchi, H.; Kobayashi, A.; Tobita, S.; Nakamura, Y. *J. Org. Chem*. **2012**, *77*, 9120. c) Yang, S.; Guan, D.; Yang, M.; Tian, J.; Chu, W.; Sun, Z. *Tetrahedron Lett*. **2015**, *56*, 2223

8) Kato, S.; Shimizu, S.; Taguchi, H.; Kobayashi, A.; Tobita, S.; Nakamura, Y. *J. Org. Chem*. **2012**, *77*, 9120.

9) a) Wang, H. Y.; Liu, F.; Xie, L. H.; Tang, C.; Peng, B.; Huang, W.; Wei, W. *J. Phys. Chem. C* **2011**, *115*, 6961. b) Niu, F.; Niu, H.; Liu, Y.; Lian, J.; Zeng, P. *RSC Adv*. **2011**, *1*, 415

10) a) Tomkeviciene, A.; Grazulevicius, J. V; Kazlauskas, K.; Gruodis, A.; Jursenas, S.; Ke, T. H.; Wu, C. C. *J. Phys. Chem. C* **2011**, *115*, 4887. b) Gong, S.; Zhao, Y.; Yang, C.; Zhong, C.; Qin, J.; Ma, D. *J. Phys. Chem. C* **2010**, *114*, 5193. c) Kanibolotsky, A. L.; Perepichkaz, I. F.; Skabara, P. J. *Chem. Soc. Rev*. **2010**, *39*, 2695.

11) Gong, W. L.; Zhong, F.; Aldred, M. P.; Fu, Q.; Chen, T.; Huang, D. K.; Shen, Y.; Qiao, X. F.; Ma, D.; Zhu, M. Q. *RSC Adv*. **2012**, *2*, 10821.

12) Kochapradist, P.; Prachumrak , N.; Tarsang, R.; Keawin, T.; Jungsuttiwong, S.; Sudyoadsuk, T.; Promarak, V. *Tetrahedron Lett.* **2013**, *54*, 3683.

13) Gong, W. L.; Wang, B.; Aldred, M. P.; Li, C.; Zhang, G. F.; Chem, T.; Wang, L.; Zhu, M. Q. *J. Mater. Chem. C* **2014**, *2*, 7001.

14) a) Liu, F.; Tang, C.; Chen, Q. Q.; Li, S. Z.; Wu, H. B.; Xie, L. H.; Peng, B.; Wei, W.; Cao, Y.; Huang, W. *Org. Electron*. **2009**, *10*, 256. b) Kumchoo, T.; Promarak, V.; Sudyoadsuk, T.; Sukwattanasinitt, M.; Rashatasakhon, P. *Chem.-Asian J*. **2010**, *5*, 2162. c) Tao, S.; Zhou, Y.; Lee, C. S.; Zhang, X.; Lee, S. T. *Chem. Mater*. **2010**, *22*, 2138. d) Ali, F.; Periasamy, N.; Patankar, M. P.; Narasimhan, K. L. *J. Phys. Chem. C* **2011**, *115*, 2462. e) Thomas, K. R. J.; Kapoor, N.; Bolisetty, M. N. K. P.; Jou, J. H.; Chen, Y. L.; Jou, Y. C. *J.*

Org. Chem. **2012**, *77*, 3921. f) Chen, S.; Wei, J.; Wang, K.; Wang, C.; Chen, D.; Liu, Y.; Wang, Y. *J. Mater. Chem. C* **2013**, *1*, 6594. g) Usluer, O. *J. Mater. Chem. C* **2014**, *2*, 8098.

15) a) Grazulevicius, J. V.; Strohriegl, P.; Pielichowski, J.; Pilichowski, K. *Prog. Plym. Sci*. **2003**, **28**, 1297. b) Morin, J. F,; Leclerc, M.; Adès, D.; Siove, A. *Macromole. Rapid Commun*. **2005**, *26*, 761.

16) a) Tsai, M. H.; Ke, T. H.; Lin, H. W.; Wu, C. C.; Chiu, S. F.; Fang, F. C.; Liao, Y. L.; Wong, K. T.; Chen, Y. H.; Wu, C. I. *ACS Appl. Mater. Interfaces* **2009**, *1*, 567. b) Tao, Y.; Wang, Q.; Yang, C.; Zhang, C.; Zhang, K.; Qin, J.; Ma, D. *Adv. Funct. Mater*. **2010**, *20*, 304. c) Mizuno, Y.; Takasu, I.; Uchikoga, S.; Enomoto, S.; Sawabe, T.; Amano, A.; Wada, A.; Sugizaki, T.; Yashida, J.; Ono, T.; Adachi, C. *J. Phys. Chem. C* **2012**, *116*, 20681. d) Cui, L. S.; Liu, Y.; Yuan, X. D.; Li, Q.; Jiang, Z. Q.; Liao, L. S. *J. Mater. Chem. C* **2013**, *1*, 8177. e) Du, X.; Huang, Y.; Tao, S.; Yang, X; Wu, C.; Wei, H.; Chan, M. Y.; Yan, V. W. W.; *Chem.-Asian J.* **2014**, *9*, 1500. f) Shi, H.; Xin, D.; Dong, X.; Dai, J. X.; Wu, X.; Miao, Y.; Fang, L.; Wang, H.; Choi, M. M. F. *J. Mater. Chem. C* **2014**, *2*, 2160. g) Cheng, S. H.; Hung, W. Y.; Cheng, M. H.; Chen, H. F.; Chaskar, A.; Lee, G. H.; Chou, S. H.; Wong, K. T. *J. Mater. Chem. C* **2014**, *2*, 8554. h) Yuan, X. D.; Liang, J.; He, Y. C.; Li, Q.; Zhang, C.; Jiang, Z. Q.; Liao, L. S. *J. Mater. Chem. C* **2014**, *2*, 8736. i) Tang, C.; Bi, R.; Tao, Y.; Wang, F.; Cao, X.; Wang, S.; Jiang, T.; Zhang, C.; Zhang, H.; Huang, W. *Chem. Commun*. **2015**, *51*, 1650. j) Rothmann, M. M.; Haneder, S.; Como, E. D.; Lennartz, C.; Schidknecht, C.; Strohriegl, P. *Chem. Mater.* **2010**, *22*, 2403. k) Wagner, D.; Hoffmann, S. T.; Heinemeyer, U.; Münster, I.; Köhler, A.; Strohriegl, P. *Chem. Mater*. **2013**, *25*, 3758. l) Bagnich, S. A.; Athanasopoulos, S.; Rudnick, A.; Schroegel, P.; Bauer, I.; Greenham, N. C.; Strohriegl, P.; Köhler, A. *J. Phys. Chem. C* **2015**, *119*. 2380. m) Sonntag, M.; Strohriegl. P. *Chem. Mater.* **2004**, *16*, 4736.

17) Huang, H.; Fu, Q.; Pan, B.; Zhuang, S; Wang, L.; Chen, J.; Ma, D.; Yang, C. *Org. Lett*. **2012**, *14*, 4786.

18) a) Boudreault, P. L. T.; Wakim, S.; Tang, M. L.; Tao, Y.; Bao, Z.; Leclerc, M. *J. Mater. Chem*. **2009**, *19*, 2921. b) Cheedarala, R. K.; Kim, G. H.; Cho, S.; Lee, J.; Kim, J.; Song, H. K.; Kim, I. Y.; Yang, C. *J. Mater. Chem*. **2011**, *21*, 843. c) Mutkins, K.; Chen, S. S.Y.; Pivrikas, A.; Aljada, M.; Burn, P. L.; Meredith, P.; Powell, B. J. *Polym. Chem*. **2013**, *4*, 916. d) Montoya, M. M.; Oritz, R. P.; Curiel, D.; Spinosa, A. E.; Allain, A.; Facchetti, A.; Marks, T. J. *J. Mater. Chem. C* **2013**, *1*, 1959. e) Tomkeviciene, A.; Grazulevicius, J. V.; Volyniuk, D.; Jankauskas, V.; Sini, G. *Phys. Chem. Chem. Phys*. **2014**, *16*, 13932. f) Sonntag, M.; Kreger, K.; Hanft, D.; Strohriegl, P. *Chem. Mater*. **2005**, *17*, 3031.

19) a) Ooyama, Y.; Nagano, T.; Inoue, S.; Imae, I.; Komaguchi, K.; Ohshita, J.; Harima, Y. *Chem.-Eur. J*. **2011**, *17*, 14837. b) Lee, W.; Cho, N.; Won, J. K.; Ko, J.; Hong, J. I. *Chem-Asian J*. **2012**, *7*, 343. c) Chu, H. C.; Sahu, D.; Hsu, C. Y.; Podhy, H.; Patra, D.; Lin, J. T.; Bhattacharya, D.; Lu, K. L.; Wei, K. H.; Lin, H. C. *Dyes Pigm*. **2012**, *94*, 1488. d) Thongkasee, P.; Thangthong, A.; Janthasing, N.; Sudyoadsuk, T.; Naumuangruk, S.; Keawin, T.; Jungsuttiwong, S.; Promarak, V. *ACS Appl. Mater. Interfaces* **2014**, *6*, 8212. e) Su, J. Y.; Lo, C. Y.; Tsai, C. H.; Chen, C. H.; Chou, S. H.; Liu, S. H.; Chou, P. T.; Wong, K. T. *Org. Lett*. **2014**, *16*, 3176. f) Pearson, A, J.; Watters, D. C.; Yi, H.; Sorjadi, M. S.; Reynolds, L. X.; Marchisio, P. P.; Kingsley, J.; Haque, S. A.; Iraqi, A.; Lidzey, D. G. *RSC Adv*. **2014**, *4*, 43142.

20) a) Venkateswrarao, A.; Thomas, K. R. J.; Lee, C. P.; Ho, K. C. *Tetrahedron. Lett*. **2013**, *54*, 3985. b) Venkateswrarao, A.; Thomas, K. R. J.; Lee, C. P.; Lee, C. T.; Ho, K. C. *ACS Appl. Mater. Interfaces* **2014**, *6*, 2528.

21) a) Zhang, Y.; Wang, L.; Wada, T.; Sasabe, H. *Macromolecules* **1996**, *29*, 1569. b) Zhang, Y.; Wang, L.; Wada, T.; Sasabe, H. *Chem. Mater*. **1997**, *9*, 2798. c) Hwang, J.; Sohn, J.; Park, S. Y. *Macromolecules* **2013**, *36*, 7970. d) Hofmann, U.; Grasruck, M.; Leopold, A.;

Schreiber, A.; Schloter, S.; Hohle, C.; Strohriegl, P.; Haarer, D.; Zilker, S. J. *J. Phys. Chem. B* **2010**, *104*, 3887.

22) a) Chang, C. C.; Wu, J. Y.; Chien, C. W.; Wu, S.; Liu, H.; Kang, C. C.; Yu, ; Chang, T. C. *Anal. Chem*. **2003**, *75*, 6177. b) Gee, H. C.; Lee, C. H.; Jeang, Y. H.; Jang, W. D. *Chem. Commun*. **2011**, *47*, 11963. c) Goswami, S.; Paul, S.; Manna, A.; *J. Chem. Soc., Dalton Trans.* **2013**, *42*, 10682. d) Feng, X. J.; Tian, P. Z.; Xu, Z.; Chen, S. F.; Wang, M. S. *J. Org. Chem*. **2013**, *78*, 11318. e) Konidena, R. K.; Thomas, K. R. J. *RSC Adv*. **2014**, *4*, 22902.

23) Jiang, H.; Sun, J. *New J. Chem*. **2013**, *37*, 3161.

24) a) Kong, K.; Xiao, L.; Liu, Y.; Chen, Z.; Qu, B.; Gong, Q. *New J. Chem*. **2010**, *34*, 1994. b) Park, Y.; Kim, B.; Lee, C.; Hyun, A.; Jang, S.; Lee, J. H.; Gal, Y. S.; Kim, J. Y.; Kim, K. S.; Park, J. *J. Phys. Chem. C* **2011**, *115*, 4843. c) Hua, Y.; Chang, S.; Huang, H.; Zhou, X.; Zhu, X.; Zhao, J.; Chen, T.; Wong, W. Y; Wong, W. K. *Chem. Mater*. **2013**, *25*, 2146. d) Yao, L.; Sun, S.; Xue, S.; Zhang, S.; Wu, X.; Zhang, H.; Pan, Y.; Gu, C.; Li, F.; Ma, Y. *J. Phys. Chem. C* **2013**, *117*, 14189-14196. e) Janaka, H.; Shizu, K.; Nakanotani, H.; Adachi, C. *J. Phys. Chem. C* **2014**, *118*, 15985. f) Tian, Q.; Yang, X.; Cheng, M.; Wong, H.; Sun, L. *J. Phys. Chem. C* **2014**, *118*, 16851. g) Huang, Z. S,; Feng, H. L.; Zong, X. F.; Iqbal, Z.; Zeng, H.; Kuang, D. B.; Wang, L.; Meier, H.; Cao, D. *J. Mater. Chem. C* **2014**, *2*, 15365. h) Bodedla, G. B.; Thomas, K. R. J.; Li, C. T.; Ho, K. C. *RSC Adv*. **2014**, *4*, 53588. i) Ananthakrishnan, J. S.; Varathan, E.; Subramanian, V.; Somanathan, N.; Mandal, A. B. *J. Phys. Chem. C* **2014**, *118*, 28084-28094. j) Lai, R. Y.; Kong, X.; Janekhe, S. A.; Bard, A. J. *J. Am. Chem. Soc*. **2003**, *125*, 12631. k) Kulkarni, A. P.; Wu, P. T.; Kwon, T. W.; Jenekhe, S. A. *J. Phys. Chem. B* **2005**, *109*, 19584. l) Kong, X.; Kulkarni, A. P.; Jenekhe, S. A. *Macromolecules* **2003,** *36,* 8992. m) Kulkarni, A. P.; Kong, X.; Jenekhe, S. A. *Macromolecules* **2006***, 39,* 8699. n) Lai, R. Y.; Fabrizio, E. F.; Lu, L.; Jenekhe, S. A.; Bard, A. J. *J. Am. Chem. Soc*. **2001**, *123*, 9112. o) Jenekhe, S. A.; Lu, L.; Alam, M. M.

Macromolecules 2001, 34, 7315. p) Reghu, R. R.; Grazulevicius, V. J.; Simokaitiene, J.; Data, P.; Karon, K.; Lapkowski, M.; Gaidelis, V.; Jankauskas, V. *J. Phys. Chem. C* **2012**, *116*, 15878.

25) Sun, J.; jiang, H. J.; Zhang, J. L.; Tao, Y.; Chen, R. F. *New J. Chem*. **2013**, *37*, 977.

26) Hauck, M.; Turdean, R.; Memminger, K.; Schönhaber, J.; Rominger, F.; Müller, T. J. J. *J. Org. Chem.* **2010**, *75*, 8591.

27) a) Franz, A. W.; Rominger, F.; Müller, T. J. J. *J. Org. Chem.* **2008**, *73*, 1795. b) Li, Y.; Feng, J. K.; Ren, A. M. *J. Org. Chem.* **2005**, *70*, 5987. c) Franz, A. W.; Popa, L. N.; Rominger, F.; Müller, T. J. J. *Org. Biomol. Chem*. **2009**, *7*, 469.

28) a) Barkschat, C. S.; Stoychera, S.; Himmelhaus, M.; Müller, T. J. J. *Chem. Mater*. **2010**, *22*, 52. b) Sailer, M.; Nonnenmacher, M.; Oesar, T.; Müller, T. J. J. *Eur. J. Org. Chem.* **2006**, 423. c) Sailer, M.; Gropeanu, R. A.; Müller, T. J. J. *J. Org. Chem*. **2003**, *68*, 7509. d) Hauck, M.; Schönhaber, J.; Zucchero, A. J.; Hardcastle, K. I.; Müller, T. J. J.; Bunz, U. H. F. *J. Org. Chem*. **2007**, *72*, 6714. e) Mayer, T.; Ogermann, D.; Pankrath. A.; Kleinermanns. K.; Müller, T. J. J. *J. Org. Chem*. **2012**, *77*, 3704. f) Krämer, C. S.; Zeitler, K.; Müller, T. J. J. *Org. Lett*. **2000**, *2*, 3723. g) Krain, M.; Oeser, T.; Müller, T. J. J. *Org. Lett*. **2008**, *10*, 2797. g) Krämer, C. S.; Müller, T. J. J. *Eur. J. Org. Chem*. **2003**, 3534. h) Krämer, C. S.; Zeitler, K.; Müller, T. J. J. *Tetrahedron Lett*. **2001**, *42*, 8619.

29) a) Stille, J. K. *Angew. Chem., Int. Ed.*, **1986**, *98*, 504. b) Daub. J.; Engl, R.; Kurzawa, S.; Miller, S. E.; Schneider, S.; Stockmann, A.; Wasielewski, M. R. *J. Phys. Chem. A* **2001**, *105*, 5655.

30) a) Morin, J. F.; Leclerc, M. *Macromolecules* **2001**, *34*, 4680. b) Morin, J. F.; Leclerc, M. *Macromolecules*. **2002**, *35*, 8413. c) Fu, Y.; Bo, Z. *Macromole. Rapid Commun.* **2005**, *26*, 1704.

31) Reichardt, C. *Chem. Rev*. **1994**, *94*, 2319.

32) Tyagi, P.; Venkateswarao, A.; Thomas, K. R. J. *J. Org. Chem*. **2011**, *76*, 4571.

33) Panthi, K.; Adhikari, R. M.; Kinstle, T. H. *J. Phys. Chem. A* **2010**, *114*, 4550.

34) Sung, J.; Kim, P.; Lee, Y. O.; Kim, J. S.; Kim, D. *J. Phys. Chem. Lett*. **2011**, *2*, 818.

35) Subuddhi, U.; Halder, S.; Sankararaman, S.; Mishra, A. K. *Photochem. Photobiol. Sci.* **2006**, *5*, 459.

36) a) Mes, G. F.; Jong, B. D.; Ramesdonk, H. J. V.; Verhoeven, J. W.; Warman, J. M.; Haas, M. P. D.; Dool, L. E. W. H. *J. Am. Chem. Soc*. 1984, 106, 6524. b) Manohara, S. R.; Udaya Kumar, V.; Shivakumaraiah, Gerward, L. *J. Molecular. Liquids* **2013**, *181*, 97.

37) Gaussian09, Revision A. 02, M. Frish, J.; Trucks, G. H.; Schlegel, H. B.; Scuseria, G. E.; Robb, M. A.; Cheseman, J. R.; Scalmani, G.; Barone, V.; Mennucci, B.; Petersson, G. A.; Nakatsuji, H.; Caricato, M.; Li, X,; Hratchian, H. P.; Izmaylov, A. F.; Bloino, J.; Zheng, G.; Snnengerg, J. L.; Hada, M.; Ehara, M.; Toyota, K.; Fukuda, R.; Hasegawa, J.; Ishida, M.; Nakajima, T.; Honda, Y.; Kitao, O.; Nakai, H.; Vreven, T.; Montgomery, J. A.; Peralta, Jr. J. E.; Ogliaro, F.; Bearpark, M.; Heyd, J. J.; Brothers, E.; Kudinm, K. N.; Staroverov, V. N.; Kobayashi, R.; Normand, J.; Raghavachari, K.; Rendell, A.; Burant, J. C.; Iyengar, S. S.; Tomasi, J.; Cossi, M.; Rega, N.; Millam, J. M.; Klene, M.; Knox, J. E.; Cross, J. B.; Bakken, V.; Adamo, C.; Jaramillo, J.; Gomperts, R.; Stratmann, R. E.; Yazyev, O.; Austin, A. J.; Cammi, R.; Pomelli, C.; Ochterski, J. W.; Martin, R. L.; Morokuma, K.; Zakrzewski, V. G.; Voth, G. A.; Salvador, P.; Dannenberg, J. J.; Dapprich, S.; Daniels, A. D.; Farkas, O.; Foresman, J. B.; Ortiz, J. V.; Cioslowski, J.; Fox, D. J. Gaussian Inc. Wallingford CT, **2009**.

38) a) Becke, A. D. *J. Chem. Phys*. **1993**, *98*, 1372. b) Lee, C.; Yang, W.; Parr, G. *Phys. Rev. B* **1988**, *37*, 785.

39) a) Marcus, R. A. *J. Chem. Phys*. **1956**, *24*, 966. b) Hush, N. S. *J. Chem. Phys.* **1958**, *28*, 962. c) Marcus, R. A. *Rev. Mod. Phys*. **1993**, *65*, 599.

40) a) Nelsen, S. F.; Wolff, J. J.; Chang, H.; Powell, D. P. *J. Am. Chem. Soc.* **1991**, *113*, 7882. b) Nelsen, S. F.; Blomgren, F. *J. Org. Chem*. **2001**, *66*, 6551.

41) a) Ran, X. Q.; Feng, J. K.; Ren, A. M.; Li, W. C.; Zou, L. Y.; Sun, C. C. *J. Phys. Chem. A* **2009**, *113*, 7933. b) Yin, J.; Chen, R. F.; Zhang, S. L.; Ling, Q. D.; Huang, W. *J. Phys. Chem. A* **2010**, *114*, 3655. c) Cias, P.; Slugovc, S.; Gescheidt, G. *J. Phys. Chem. A* **2011**, *115*, 14519. d) Yao, Y. Tao, M. K.; Chen, R. F.; Zheng, C.; An, Z. F.; Huang, W. *RSC Adv*. **2012**, *2*, 7860. e) Varathan, E.; Vijay, D.; Kumar, P. S. V.; Subramanian, V. *J. Mater. Chem. C* **2013**, *1*, 4261. f) Varathan, V.; Vijay, D; Subramanjan, V. *J. Phys. Chem. C* **2014**, *118*, 21741.

42) a) Vetrichelvan, M.; Nagarajan, R.; Veliyaveettil, S. *Macromolecules* **2006**, *39*, 8303. b) Zheng, Q.; Chen, S.; Zhang, B.; Wang, L.; Tang, C.; Katz, H. E. *Org. Lett.* **2011**, *13*, 324.